

Interaction between IGFBP-5 and TNFR1

Eun Jung Kim,^a Mi Suk Jeong,^a Jae Ryoung Hwang,[†] Je-Ho Lee,[†] and Se Bok Jang^{*}

Department of Molecular Biology, College of Natural Sciences, Pusan National University, Busan 609-735, Korea

^{*}E-mail: sbjang@pusan.ac.kr

[†]Molecular Therapy Research Center, Sungkyunkwan University, Seoul 135-710, Korea

Received April 19, 2010, Accepted May 31, 2010

Insulin-like growth factor binding protein 5 (IGFBP-5) plays an important role in controlling cell survival, differentiation and apoptosis. Apoptosis can be induced by an extrinsic pathway involving the ligand-mediated activation of death receptors such as tumor necrosis factor receptor 1 (TNFR1). To determine whether IGFBP-5 and TNFR1 interact as members of the same apoptosis pathway, recombinant IGFBP-5 and TNFR1 were isolated. The expression and purification of the full-length TNFR1 and truncated IGFBP-5 proteins were successfully performed in *E. coli*. The binding of both IGFBP-5 and TNFR1 proteins was detected by surface plasmon resonance spectroscopy (BIAcore), fluorescence measurement, electron microscopy, and size-exclusion column (SEC) chromatography. IGFBP-5 indeed binds to TNFR1 with an apparent K_D of 9 nM. After measuring the fluorescence emission spectra of purified IGFBP-5 and TNFR1, it was found that the tight interaction of these proteins is accompanied by significant conformational changes of one or both. These results indicate that IGFBP-5 acts potently as a novel ligand for TNFR1.

Key Words: Truncated IGFBP-5, TNFR1, Interaction, Apoptosis

Introduction

The insulin-like growth factor (IGF) system consists of the growth factors IGF-I and IGF-II, the IGF-I and IGF-II/M-6-P receptors, IGF-binding proteins (IGFBPs), IGFBP cleaving proteases and an acid-labile subunit (ALS). IGF-I and IGF-II exhibit a broad range of effects on embryonic and fetal growth, development and metabolism.¹ IGFs mediate their pleiotropic activities by binding to and activating IGF receptors. IGF action is modulated by a group of six IGF-binding proteins that form high-affinity complexes with both IGF-I and IGF-II.^{2,3} The affinity of IGFBPs for IGFs is controlled by a variety of factors, including phosphorylation, glycosylation, and most importantly, specific proteolysis.⁴

The insulin-like growth factor binding protein 5 (IGFBP-5) is a member of the family of high-affinity binding proteins that modulates the mitogenic and anti-apoptotic effects of IGFs. Many groups have demonstrated that IGFBP-5 has IGF-independent cytostatic and cytotoxic effect on the growth of human breast^{5,8} and prostate⁹ cancer cells. IGFBP-5 translocates to the nucleus of breast cancer cells^{10,11} where it has variable effects on growth and survival when added exogenously.¹² The existence of a receptor for IGFBP-5 has been postulated as well.¹³⁻¹⁵ However, how these intrinsic growth effects of IGFBPs are mediated is largely unclear.

Tumor necrosis factor (TNF) is as an important immunity-modulating cytokine that is required for human body defense against infectious diseases and carcinogenesis.¹⁶ However, excess TNF causes various autoimmune diseases such as rheumatoid arthritis, Crohn's disease and ulcerative colitis.¹⁷⁻¹⁹ Members of the TNF ligand family exert their biological functions *via* interaction with cognate membrane receptors, which com-

prise the TNF receptor (TNFR) family.²⁰ The cytoplasmic domain of TNFR1 contains a C-terminal stretch of approximately 70 amino acids called the death domain (DD). This domain is responsible for signaling apoptosis, for activation of the transcription factor NF- κ B, and for initiating mitogen-activated protein kinase (MAPK) cascades.^{21,22} TNF binding leads to trimerization of the receptors, resulting in clustering of intracellular DDs. Aggregated DDs, in turn, recruit other DD-containing adapter molecules such as TNFR1-associated DD (TRADD),²³ receptor-interacting protein²⁴ and FAS-associated DD (FADD).²⁵ This illustrates the importance of the DD as a protein-protein interaction domain in the formation of a functional TNFR1 signaling complex.

TNF-alpha is a ligand of TNFR1 that upon binding triggers a series of intracellular events initiated by the recruitment of a key TRADD adaptor protein to the receptor complex. IGFBP-5 binds to extracellular IGFs and modulates IGF actions on cell proliferation, differentiation, survival, and motility. Several IGFBP-5 interacting proteins have been identified such as extracellular matrix proteins.²⁶ Hwang *et al.* showed that the binding of IGFBP-5 with TNFR1 *in vivo* (unpublished work). To determine whether IGFBP-5 and TNFR1 interact as members of the same apoptosis pathway, recombinant IGFBP-5 and TNFR1 were isolated and purified. We show through a series of biochemical and biophysical measurements that IGFBP-5 interacts with TNFR1 *in vitro*. These results indicate that IGFBP-5 acts as a novel ligand of TNFR1 that can be blocked by TNF-alpha. This study therefore may provide important clues for the structural identification of apoptotic signaling pathways involving the IGFBP-5 and TNFR1 proteins.

Materials and Methods

Protein cloning, expression, and extraction. Truncated IGF

^aThese authors contributed equally to this article.

BP-5 (111-272 aa) and full-length TNFR1 (1-455 aa) were both subcloned into the C-terminal His-tagged fusion protein vector pET-28a. TNFR1 was amplified by PCR with oligonucleotides incorporating the *Bam*HI and the *Xho*I sites on the 5' primer and 3' primer containing a stop codon.

5' - GGATCCAGAAGAGAGATAGTGTGTGT - 3'
5' - CTCGAGTTATTATCTGAGAAGACTGGGC - 3'

A PCR reaction was sustained for 30 cycles, with denaturing at 94 °C for 1 min, annealing at 58 °C for 1 min, and extension at 72 °C for 1 min. The positive His₆-TNFR1 expression plasmid was identified by restriction endonuclease digestion and further verified by DNA sequencing on a Macrogen automatic DNA sequencer. The constructs were transformed into the expression host *Escherichia coli* BL21(DE3)RIL. A single colony was inoculated into 20 mL of LB (Luria-Bertani) media containing 50 µg/mL of kanamycin, and bacteria were grown at 37 °C overnight. These cells were added to four 2-L flasks, each containing 500 mL of LB and 100 µg/mL of kanamycin. The cultures were grown at 37 °C until an OD₆₀₀ of 0.5 was reached. The expression of these proteins was induced with 1 mM isopropyl-thio-β-D-galactopyranoside (IPTG). Bacterial cells were induced for 4 - 6 hours at 25 °C, and then harvested by centrifugation at 4,500 rpm for 25 min. The cell pellets were either immediately used or stored frozen at -70 °C. The IGFBP-5 and TNFR1 cell pellets were then resuspended in lysis buffer A (50 mM Tris-HCl [pH 7.5], 200 mM NaCl, and 1 mM DTT). After sonication of the cell suspensions on ice (Branson Sonifier 450), the resulting cell lysates were centrifuged at 13,500 rpm for 45 min to remove insoluble cellular debris. The insoluble fractions were directly resuspended in 2 × SDS loading buffer followed by incubation at 95 °C for 5 min. The soluble and insoluble fractions were fractionated on 15% SDS-PAGE gels and visualized by Coomassie blue staining. The supernatants were collected and used for protein purification.

Purification. His-tagged fusion proteins IGFBP-5 and TNFR1 were both applied to a Ni-NTA (Amersham Pharmacia Biotech) column for purification. The supernatants obtained from the protein extraction step were loaded onto the Ni-NTA column and pre-equilibrated with buffer A. All buffers were filtered with a 0.45-µm minisart membrane filter prior to use. The column was washed with buffer A containing imidazole, and elution of the bound protein was achieved by varying the amount of imidazole from 20 mM to 200 mM. Protein elution was monitored at 280 nm, and the resulting fractions were analyzed by electrophoresis on a 15% SDS-PAGE gel. Gel filtration was then performed using a Superdex 75 column on an HPLC system. The proteins were loaded onto a column equilibrated with buffer A and separated at a flow rate of 1.5 mL/min.

Protein determination. Protein concentrations were measured by a BioPhotometer using an UVette with a 10 mm optical path and by Bradford assay with a Bio-Rad protein Assay Kit (Bio-Rad) using bovine serum albumin as a standard.

MALDI-MS analysis. For in-gel digestion, 10 µL of trypsin solution (2 ng/L in 25 mM ammonium bicarbonate [pH 8.0]) was added and digested overnight at 37 °C. Peptides were extracted with 50% ACN/0.2% TFA (trifluoroacetic acid) and

dried under vacuum for 2 h, followed by reconstruction with 3 µL of CHCA (α -cyano-4-hydroxycinnamic acid) matrix solution (8 mg of CHCA in 1 mL of 50% ACN/0.2% TFA).²⁷ One microliter of reconstructed sample was loaded onto a 96 × 2 MALDI plate. The peptide mass was acquired with the Voyager DE-PRO (Applied Biosystems, Framingham, MA) in reflector mode under 20,000 V of accelerating voltage, 76% grid voltage and 0.002% guide-wire voltage. The Cal Mix 2 of the MALDI-MS calibration kit (Applied Biosystems, Framingham, MA) was used for the external calibration, and autolysis fragments of trypsin were used for the internal calibration. Peptide matching and protein identification were performed using the Mascot peptide mass fingerprint.

Circular dichroism (CD) measurement. Circular dichroism (CD) measurements were taken by a spectropolarimeter (JASCO J-815) in a 0.1 cm cell at 0.2 nm intervals at 25 °C. The CD spectra of the purified IGFBP-5 and TNFR1 proteins were recorded in the range of 190 - 260 nm. Each spectrum was the average of 3 scans. Far-UV CD spectra were taken using a protein concentration of 0.5 mg/mL. The CD spectra were obtained in milli-degrees and were converted to molar ellipticity prior to secondary structure analysis using the CDNN program (Gerald, B. CD spectroscopy Deconvolution, version 2.1, 1997).

BIAcore biosensor analysis. Measurements of the apparent dissociation constants (K_D) between IGFBP-5 and TNFR1 were carried out using a BIAcore 2000 biosensor (Biosensor, Sweden). TNFR1 (500 µg/mL in 10 mM sodium acetate [pH 4.0]) was covalently bound by an amine-coupling method to the carboxylated dextran matrix at a concentration corresponding to -1,200 response units (RU), as suggested by the manufacturer. A flow path involving two cells was employed to simultaneously measure the kinetic parameters from one flow cell containing the TNFR1-immobilized sensor chip to the other flow cell containing an underivatized chip. For kinetic measurements at room temperature, IGFBP-5 samples ranging in concentration from 63 to 500 nM were prepared by dilution in HBS buffer (150 mM NaCl, 3 mM EDTA, 0.005% surfactant P20, and 10 mM HEPES [pH 7.4]). Each sample was injected with 50 µL of IGFBP-5 solution into the flow cells (association phase) at a rate of 10 µL/min. Among the cycles, the immobilized ligand was regenerated by injecting 30 µL of 50 mM NaOH at a rate 10 µL/min.

Fluorescence spectroscopy. Fluorescence emission spectra were obtained using an Edinburgh (UK) FLS920 TCSPC (Time Correlated Single Photon Counting Spectrometer) with 1 cm path length cuvettes containing excitation and emission slits 20 nm in width. The fluorescence emission spectra of IGFBP-5 and TNFR1 were obtained in order to identify characteristic chemical structures, namely double bonds and aromatic groups. The emission intensity was recorded from 305 to 465 nm with an excitation wavelength of 295 nm. IGFBP-5 and TNFR1 were preincubated together for 25 min at 25 °C. The concentration of each protein was 5 µM. All spectra were obtained at a protein concentration 50 µg/mL at 24 °C. Ten spectra of each protein sample were accumulated, averaged and subjected to baseline correction by subtracting the buffer spectrum.

Electron microscopy. IGFBP-5 and TNFR1 proteins were adsorbed onto glow a thin carbon foil and negatively stained

with 2% uranyl acetate for 1 min. Images were recorded on a CCD camera with a Tecnai G2 Spirit electron microscope at a magnification of 42,000 x.

Results

IGF-binding proteins (IGFBPs) have three distinct domains (N, L, and C regions) all of which are approximately equal in size (Fig. 1A). The amino acid sequences of the seven IGFBP family members are compared in Figure 1B. The conserved residues are colored in dark gray. IGFBPs contain 240 - 328 amino acid residues and IGFBP-5 consists of 272 residues with signal peptides. All IGFBPs share similar domain organization. The highest areas of conservation are found in the N-(residues 1 to 101) and C-(from residue 189) terminal cysteine-rich regions. Compared to the N and C regions, the L-region of IGF

BP-5 is less conserved. However, structural characterization studies have revealed glycosylation and serine phosphorylation sites for IGFBP-5 in the L-region. Eleven conserved cysteines are found in the N-terminal domain and five in the C-terminal domain. The central, weakly conserved part (L-domain) contains most of the cleavage sites for specific proteases. Several different fragments of IGFBPs have been described and biochemically characterized so far.^{28,29} The secondary structure of the IGFBP-5 was predicted.

Full-length TNFR1 and truncated IGFBP-5 (111-272) including L-region and C-terminal domain proteins were expressed mainly in soluble form at 25 °C in *E. coli* BL21(DE3). The IGFBP-5 and TNFR1 proteins were expressed at high levels by the pET-28a system and were purified by Ni-NTA column chromatography. Isolated IGFBP-5 and TNFR1 had observed molecular weights of approximately 24 kDa and 50 kDa, respectively. We successfully obtained soluble proteins with final concentrations of 6 mg/mL for IGFBP-5 and 11 mg/mL for TNFR1 using a quantification kit with bovine serum (Fig. 2A and C). The soluble TNFR1 and IGFBP-5 proteins were purified to homogeneity and their identities were determined by MALDI-MS. MALDI-TOF studies revealed the approximate molecular mass of the recombinant protein, and this result was in accordance with the theoretical mass predictions for the TNFR1 and

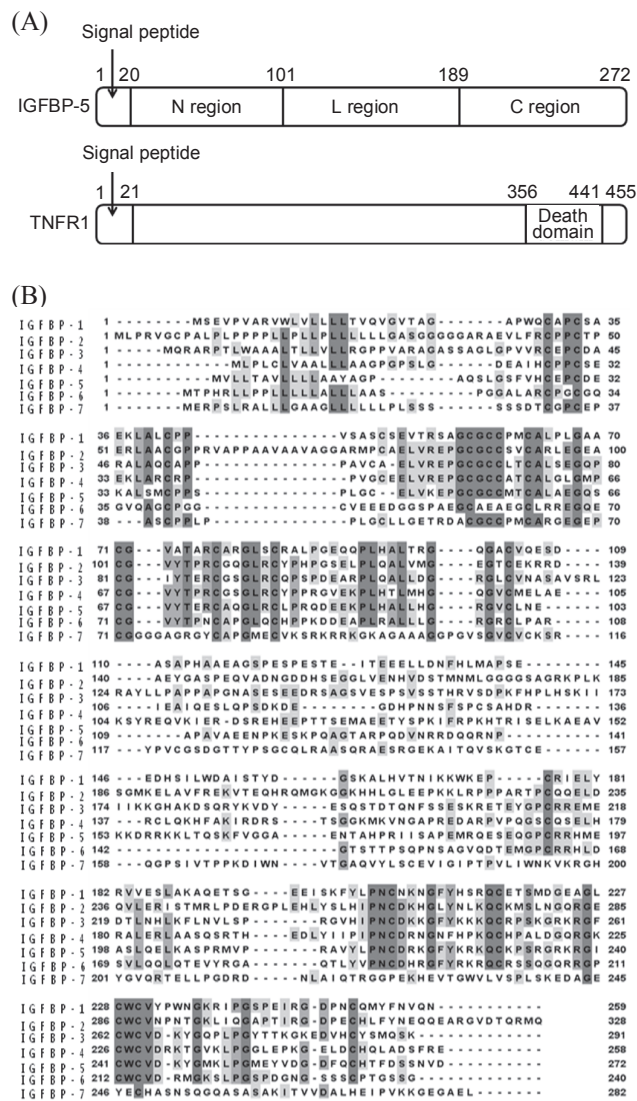


Figure 1. Domain structure, sequence alignment of IGFBPs, and predicted secondary structure of IGFBP-5. (A) Schematic diagram showing the domains of IGFBP-5 and TNFR1. (B) Sequence alignment of the core regions of human IGFBPs. The residues that are identically conserved in more than four species are in dark gray. The sequences were aligned using Jalview.

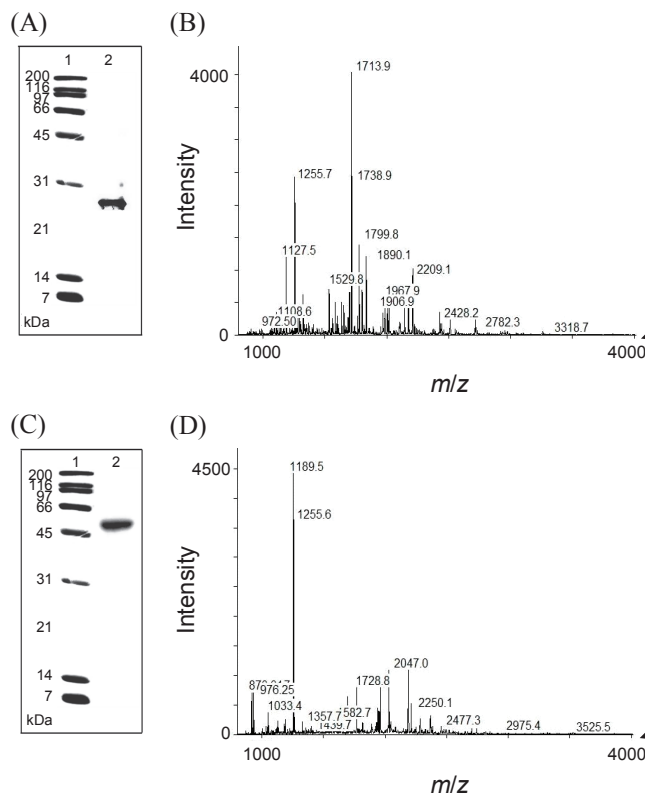


Figure 2. SDS-PAGE of the soluble IGFBP-5 and TNFR1 proteins, and MALDI-TOF mass spectra. (A) Purified, truncated IGFBP-5 and (C) full-length TNFR1 proteins are subjected to 15% SDS-PAGE following Coomassie blue staining. (B) and (D) IGFBP-5 and TNFR1 MALDI-TOF mass spectra. Peptide mixtures obtained after in-gel trypsin digestion of the excised IGFBP-5 and TNFR1 bands from the SDS-PAGE gel were analyzed by MALDI-TOF MS. The mass spectra for the tryptic digest of the bands are shown.

IGFBP-5 proteins with peptide mass tolerance (50 ppm) (Fig. 2B and D). Mass fingerprinting analysis was carried out by subjecting the protein to trypsin digestion. The monoisotopic masses obtained for the individual peptides were in the range of 800 - 3000 Da. The sequences of the digested peptides (Accession No. P19438 and pI 6.23; molecular weight, 50 kDa for TNFR1 and Accession No. P24593 and pI 8.58; molecular weight, 24 kDa for the IGFBP-5) were matched with the protein sequences in the database using the PROFOUND program.

We showed that IGFBP-5 interacts strongly with TNFR1 *in vitro* by a series of biochemical and biophysical measurements. The purified IGFBP-5 and TNFR1 proteins were mixed in a 1:1 molar ratio. After incubation for 12 hrs at 4 °C, the mixture was loaded onto a Superdex 200 HR 10/30 size-exclusion column (SEC) (Amersham Pharmacia Biotech). Binding between IGFBP-5 and TNFR1 was detected by SDS-PAGE (Fig. 3A). To further investigate the interaction between IGFBP-5 and TNFR1, the binding affinity of IGFBP-5 for TNFR1 was estimated by surface plasmon resonance spectroscopy (BIAcore) (Fig. 3B). Sensorgrams of IGFBP-5 binding to TNFR1 were used to calculate kinetic binding constants. Background sensorgrams were then subtracted from the experimental sensorgrams to yield representative specific binding constants. We found that IGFBP-5 indeed binds to TNFR1 with an apparent K_D of 9 nM.

The fluorescence emission spectra of the purified IGFBP-5 and TNFR1 proteins were confirmed, and the λ_{max} curve was found at 330 nm. The spectrum of the IGFBP-5 and TNFR1 complex was a little higher than that of TNFR1. Simply combining the spectra of IGFBP-5 and TNFR1 does not equal the spectrum of the IGFBP-5 and TNFR1 complex. The spectra display unusual emissions consistent with the solvent-inaccessible environment created by tryptophan. The fluorescence intensity of TNFR1 was highly increased by the exposed tryptophan residues. Full-length TNFR1 has five tryptophan residues whereas truncated IGFBP-5 has only one. The fluorescence intensity is about 2,000 N for IGFBP-5, but it is 3,800 N for TNFR1. At 24 °C, a small increase in fluorescence intensity occurs when IGFBP-5 and TNFR1 were mixed together in a 1:1 molar ratio at 5 μ M each (Fig. 3C). A tight interaction is most likely accompanied by significant conformational changes in either one or both proteins, an event likely to be facilitated at room temperature since the residues of aromatic groups are buried within the three-dimensional protein structure. Further, the less rigid, hydrophobic environment required for the conformational change of IGFBP-5 and TNFR1 can be initiated by a decrease in fluorescence intensity.

To examine the effects of temperature and pH on protein stability, IGFBP-5 and TNFR1 were incubated at varying temperatures (0 - 55 °C) and pH (4.5 - 9.5) for 5 min (Fig. 4A and B). The amount of soluble protein after incubation was quantified by a BioPhotometer at 280 nm. Both proteins showed optimal stability at 55 °C. The optimum pH for IGFBP-5 and TNFR1 was 7.5. This matched the pH of the buffer used for elution.^{30,31}

The folding properties of both the IGFBP-5 and TNFR1 proteins were characterized by CD spectroscopy. To determine the natures of the secondary structural elements of IGFBP-5 and TNFR1, far-UV CD spectra were recorded and analyzed

(Fig. 4C and D). The secondary structural elements and conformational properties of IGFBP-5 were somewhat different from those of TNFR1. The CD spectrum of purified IGFBP-5 exhibited three negative maxima at 203, 207 and 211 nm, whereas that of purified TNFR1 exhibited two negative maxima at 210 and 220 nm. IGFBP-5 protein is mainly β -sheet structure while TNFR1 protein is presumed to be an α -helical structure. Deconvolution of the spectra using the CDNN program indicated the following secondary structure contents: for folded IGFBP-5, 13.4% α -helices, 39.7% β -sheets, 15.6% turns and 31.3% non-ordered forms; whereas for folded TNFR1, 30.7%

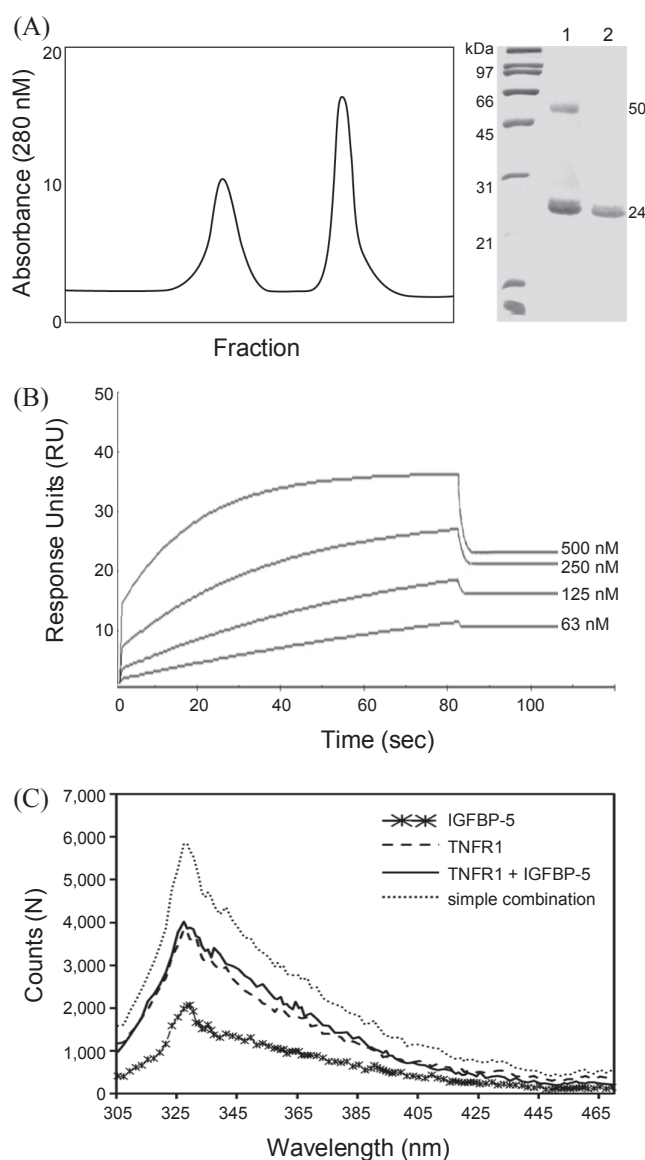


Figure 3. (A) Showing the separated fractions of protein (left panel) and binding of the IGFBP-5 and TNFR1 complex as in SDS-PAGE analysis from the size-exclusion column binding lanes 1-2 (right panel). The complex eluted earlier than IGFBP-5, whereas the peak from excess IGFBP-5 came much later. (B) BIAcore biosensor analysis of IGFBP-5 binding to TNFR1 at 25 °C. The sensorgrams for 63, 125, 250 and 500 nM human IGFBP-5 are shown. (C) Fluorescence analysis of IGFBP-5 binding to TNFR1. Fluorescence spectra of the IGFBP-5: TNFR1 complex, of the simple combination of IGFBP-5 and TNFR1, and of each individual protein are shown.

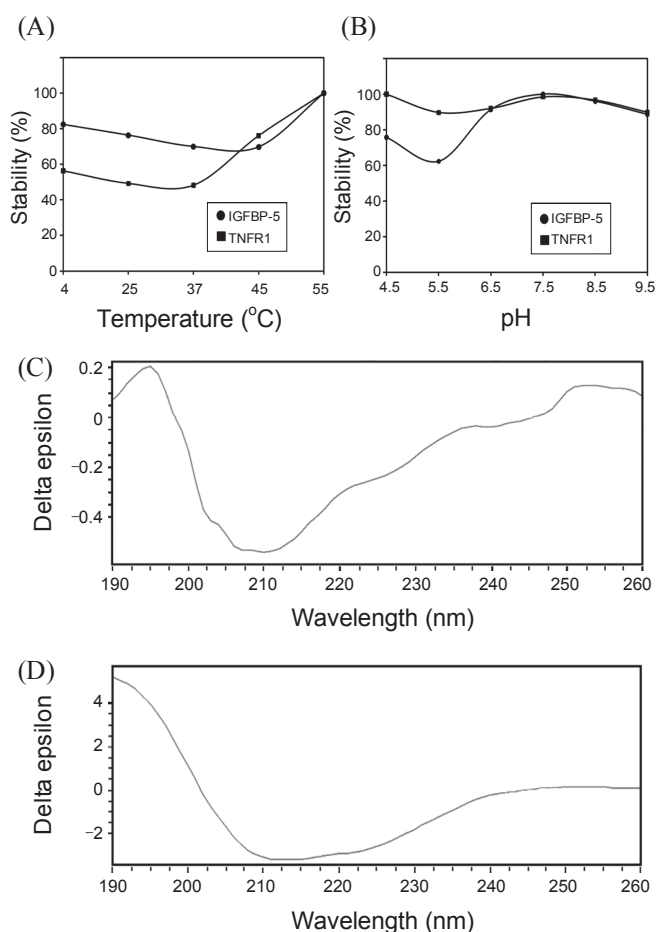


Figure 4. IGFBP-5 and TNFR1 stabilities at varying temperatures and pH. (A), (B) The protein stability reactions were carried out for 5 min at varying temperatures and pHs at a wavelength of 280 nm. The buffer for experiments contained 50 mM Tris-HCl [pH 7.5], 200 mM NaCl and 1 mM DTT. At 55 °C and pH 7.5, the optimum stabilities are shown. (C), (D) Far-UV CD spectra of IGFBP-5 and TNFR1. The CD spectrum was measured from 190 to 260 nm, and the CD signal was merged into CDNN. The experiment was carried out using a JASCO J-715 spectropolarimeter with a 0.1 cm cell at 0.2 nm intervals and 25 °C. These spectra were the result of 3 scans.

α -helices, 19.3% β -sheets, 17% turns and 33% non-ordered forms.

To define the oligomerization numbers and shapes of IGFBP-5 and TNFR1, we performed electron microscopy (EM) on IGFBP-5 and TNFR1 complex and TNFR1 only (Fig. 5A and B). Images of negatively stained proteins were recorded, and the complex was shown to be homogeneous in size and overall shape, suggesting that the particles adsorbed to the carbon support film according to a preferred orientation. TNFR1 molecules and the complex with IGFBP-5 showed propeller-like shapes. In the TNFR1 only structure, the holes of propeller-like shape are more opened. In contrast, some particles of IGFBP-5 and TNFR1 complex showed as closing the holes by the binding of IGFBP-5 ligand.

Discussion

Apoptosis was induced by an extrinsic pathway involving

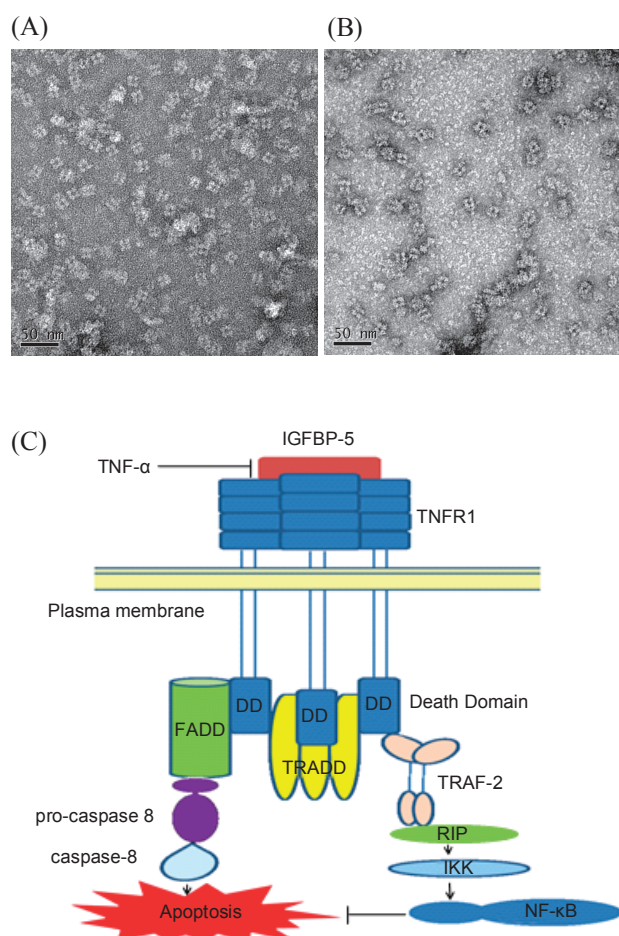


Figure 5. (A), (B) Visualization of IGFBP-5 and TNFR1 propeller-like shaped complexes and TNFR1 only by electron microscopy. Electron micrograph area of IGFBP-5 and TNFR1 were negatively stained with 2% uranyl acetate for 1 min. The scale bar is 50 nm. (C) Overview of the IGFBP-5 signaling pathway involved in apoptosis. IGFBP-5 acts as a novel TNFR1 ligand.

the ligand-mediated activation of death receptors such as TNF receptor 1 (TNFR1). Upon binding of TNF- α to TNFR1, an intracellular death effector complex is formed consisting of adaptor molecules such as Fas-associated death domain (FADD) protein and an inactive precursor form of caspase-8.³² Formation of this complex leads to the cleavage of caspase-8 into active subunits and the subsequent proteolysis of downstream substrates. Activation of the transcription factor nuclear factor- κ B (NF- κ B) by nuclear translocation elicits a potent survival signal that blocks this death receptor-mediated apoptotic pathway.³³

In the present study, we show the purification and characterization of the truncated IGFBP-5 and full-length TNFR1 proteins in *E. coli*. Further, we confirmed by a series of biochemical and biophysical measurements that IGFBP-5 interacts strongly with TNFR1 *in vitro*. Intriguingly, IGFBP-5 binds with high affinity to TNFR1. TNF- α is a ligand of TNFR1 that, upon binding, triggers a series of intracellular events initiated by the recruitment of a key TNFR1-associated death domain protein (TRADD) adaptor protein to the receptor complex. These results indicate that IGFBP-5 acts potently as a novel ligand of TNFR1 that can be blocked by TNF- α (Fig. 5C). This study

therefore may provide important clues for the structural identification of apoptotic signaling pathways involving the IGFBP-5 and TNFR1 proteins.

Acknowledgments. This study was supported by the National R&D Program for Cancer Control, Ministry of Health & Welfare, Republic of Korea (0720110) to S.B.J. and by Pusan National University in program Post-Doc. 2010 to M.S.J.

References

1. Stewart, C. E.; Rotwein, P. *Physiol. Rev.* **1996**, *76*, 1005-1026.
2. Clemmons, D. R. *Cytokine Growth Factor Rev.* **1997**, *8*, 45-62.
3. Rajaram, S.; Baylink, D. J.; Mohan, S. *Endocr. Rev.* **1997**, *18*, 801-831.
4. Conover, C. A. *Prog. Growth Factor Res.* **1995**, *6*, 301-309.
5. Butt, A. J.; Dickson, K. A.; McDougall, F.; Baxter, R. C. *J. Biol. Chem.* **2003**, *278*, 29676-29685.
6. Butt, A. J.; Firth, S. M.; King, M. A.; Baxter, R. C. *J. Biol. Chem.* **2000**, *275*, 39174-39181.
7. Butt, A. J.; Fraley, K. A.; Firth, S. M.; Baxter, R. C. *Endocrinology* **2002**, *143*, 2693-2699.
8. Gill, Z. P.; Perks, C. M.; Newcomb, P. V.; Holly, J. M. P. *J. Biol. Chem.* **1997**, *272*, 25602-25607.
9. Rajah, R.; Valentinis, B.; Cohen, P. *J. Biol. Chem.* **1997**, *272*, 12181-12188.
10. Schedlich, L. J.; Le Page, S. L.; Firth, S.; Briggs, L. J.; Jans, D. A.; Baxter, R. C. *J. Biol. Chem.* **2000**, *275*, 23462-23470.
11. Schedlich, L. J.; Young, T. Y.; Firth, S. M.; Baxter, R. C. *J. Biol. Chem.* **1998**, *273*, 18347-18352.
12. McCaig, C.; Perks, C. M.; Holly, J. M. *J. Cell Sci.* **2002**, *115*, 4293-4303.
13. Address, D. L. *J. Biol. Chem.* **1995**, *270*, 28289-28296.
14. Address, D. L. *Am. J. Physiol.* **1998**, *274*, E744-E750.
15. Oh, Y.; Muller, H. L.; Pham, H.; Rosenfeld, R. G. *J. Biol. Chem.* **1993**, *268*, 26045-26048.
16. Aggarwal, B. B. *Nat. Rev. Immunol.* **2003**, *3*, 745-756.
17. Feldmann, M.; Maini, R. N. *Nat. Med.* **2003**, *9*, 1245-1250.
18. Kooloos, W. M.; de Jong, D. J.; Huizinga, T. W.; Guchelaar, H. *J. Drug Discov.* **2007**, *12*, 125-131.
19. Rutgeerts, P.; Assche, G. V.; Vermeire, S. *Gastroenterology* **2004**, *126*, 1593-1610.
20. Locksley, R. M.; Killeen, N.; Lenardo, M. J. *Cell* **2001**, *104*, 487-501.
21. Tartaglia, L. A.; Ayres, T. M.; Wong, G. H. W.; Goeddel, D. V. *Cell* **1993**, *74*, 845-853.
22. Boone, E.; Vansvoorde, V.; De Wilde, G.; Haegeman, G. *FEBS Lett.* **1998**, *441*, 275-280.
23. Hsu, H.; Xiong, J.; Goeddel, D. V. *Cell* **1995**, *81*, 495-504.
24. Stanger, B. Z.; Leder, P.; Lee, T. H.; Kim, E.; Seed, B. *Cell* **1995**, *81*, 513-523.
25. Chinnaiyan, A. M.; O'Rourke, K.; Tewari, M.; Dixit, V. M. *Cell* **1995**, *81*, 505-512.
26. Qijin, X.; Ben, Y.; Shenghua, L.; Cunming, D. *J. Biol. Chem.* **2004**, *279*, 4269-4277.
27. Gharahdaghi, F.; Weinberg, C. R.; Meagher, D. A.; Imai, B. S.; Mische, S. M. *Electrophoresis* **1999**, *20*, 601-605.
28. Spencer, E. M.; Chan, K. *Prog. Growth Factor Res.* **1995**, *6*, 209-214.
29. Wajant, H.; Pfizenmaier, K.; Scheurich, P. *Cell Death and Differentiation* **2003**, *10*, 45-65.
30. Hong, J.; Jeong, M. S.; Kim, J. H.; Kim, B. G.; Holbrook, S. R.; Jang, S. B. *Bull. Korean Chem. Soc.* **2008**, *29*, 381-388.
31. Ha, J. H.; Jeong, M. S.; Jo, W.; Jeong, M.; Jang, S. B. *Bull. Korean Chem. Soc.* **2010**, *2*, 275-280.
32. Ashkenazi, A.; Dixit, V. M. *Science* **1998**, *281*, 1305-1308.
33. Beg, A. A.; Baltimore, D. *Science* **1996**, *274*, 782-787.